

See discussions, stats, and author profiles for this publication at: <https://www.researchgate.net/publication/12015453>

# Electric Manipulation of Bioparticles and Macromolecules on Microfabricated Electrodes

ARTICLE *in* ANALYTICAL CHEMISTRY · MAY 2001

Impact Factor: 5.64 · DOI: 10.1021/ac001109s · Source: PubMed

---

CITATIONS

128

---

READS

30

9 AUTHORS, INCLUDING:



[Michael J Heller](#)

University of California, San Diego

83 PUBLICATIONS 2,589 CITATIONS

SEE PROFILE

# Electric Manipulation of Bioparticles and Macromolecules on Microfabricated Electrodes

Ying Huang,\* Karla L. Ewalt,<sup>†</sup> Marcus Tirado, Robert Haigis, Anita Forster, Donald Ackley,<sup>‡</sup> Michael J. Heller, James P. O'Connell, and Michael Krihak

Nanogen Inc., 10398 Pacific Center Court, San Diego, California 92121

**Bioparticle separation, bioparticle enrichment, and electric field-mediated immune detection were carried out on microfabricated semiconductor chips utilizing ac and dc electric fields. Microscale separation on a chip surface having an active area of  $\sim 16 \text{ mm}^2$  was demonstrated for a mixture of *Bacillus globigii* spores and *Escherichia coli* bacteria. Dielectrophoretic enrichment was performed by collecting target bioparticles from a flow stream in flow cells of  $\sim 7.5 \text{ }\mu\text{L}$ , achieving a 20-fold increase in the concentration of *E. coli* bacteria from a diluted sample, a 28-fold enrichment for peripheral blood mononuclear cells from red blood cells, and a 30-fold increase in white blood cells from diluted whole blood. The ability to manipulate and collect bioparticles and macromolecules at microfabricated electrodes with ac and dc fields was further illustrated in electric field-mediated immunoassays for analyzing the biological identities of *E. coli* bacteria and *B. globigii* spores. According to these results, the electric methods for manipulating bioparticles present themselves as viable techniques for novel biomedical applications in sample preparations and biochemical assays on microelectrode arrays.**

The current methods commonly used in biological laboratories for manipulation, concentration, and separation of bioparticles and macromolecules include optical tweezers,<sup>1</sup> fluorescence<sup>2</sup> or magnetic activated cell sorting,<sup>3,4</sup> centrifugation,<sup>5</sup> filtration,<sup>6</sup> and electric field-based manipulations and separations.<sup>7–9</sup> Among these methods, the electric field-based approach is well suited for miniaturiza-

tion because of relative ease of microscale generation and structuring of an electric field on microchips. Furthermore, electrically driven microchips provide the advantages of speed, flexibility, controllability, and ease of application to automation.

Depending on the nature of bioparticles to be manipulated, different types of electric fields can be applied: (1) a dc field for electrophoresis (EP) of *charged* bioparticles;<sup>8</sup> (2) a nonuniform ac field for dielectrophoresis (DEP) of *polarized* (charged or neutral) bioparticles;<sup>9–12</sup> (3) the combined ac and dc fields for manipulating charged and neutral bioparticles. On the microchip scale, EP has been used in conjunction with electro-osmosis for electrokinetic transportation and separation of molecules and cells in microchannels<sup>13–17</sup> and has been exploited to manipulate and concentrate charged molecules to specified locations on microchips for accelerated DNA hybridization and electronic stringency.<sup>18–21</sup> Because most biological cells have similar electrophoretic mobilities,<sup>8</sup> EP for manipulation of cells has limited applications. On the other hand, DEP has been successfully applied on microchip scales to manipulate and separate a variety of biological cells<sup>22–26</sup> including bacteria, yeast, and mammalian cells. Because the DEP forces exerted on particles are proportional

\* Corresponding author. Phone: (858) 410-4979. Fax: (858) 410-4650. E-mail: yhuang@nanogen.com.

<sup>†</sup> Current address: The Scripps Research Institute, 10550 North Torrey Pines Rd., La Jolla, CA 92037.

<sup>‡</sup> Current address: Redeon, Inc. 124 Mt. Auburn St., Cambridge, MA 02138.

- (1) Weber, G.; Greulich, K. *Int. Rev. Cytol.* **1990**, *133*, 1–41.
- (2) Villas, B. H. *Cell Vision* **1998**, *5*, 56–61.
- (3) Handgretinger, R.; Lang, P.; Schumm, M.; Taylor, G.; Neu, S.; Koscielna, E.; Niethammer, D.; Klingebiel, T. *Bone Marrow Transplant.* **1998**, *21*, 987–993.
- (4) Marvrou, A.; Colialexi, A.; Tsangaris, G. T.; Antsaklis, A.; Panagiotopoulou, P.; Tsengghi, C.; Metaxotoy, C. *In Vivo* **1998**, *12*, 195–200.
- (5) Bauer, J. J. *Chromatogr., B* **1999**, *722*, 55–69.
- (6) Cheng, J.; Kricka, L. J.; Sheldon, E. L.; Wilding, P. In *Mirosystem Technology in Chemistry and Life Science*; Manz, A., Becker, H., Eds.; Topics in Current Chemistry 194; Springer-Verlag: Heidelberg, Germany, 1998; pp 215–231.
- (7) Volkmuth, W. D.; Austin, R. H. *Nature* **1992**, *358*, 600–602.
- (8) Bauer, J., Ed. *Cell Electrophoresis*; CRC Press: Boca Raton, FL 1994.
- (9) Jones, T. B. *Electromechanics of Particles*; Cambridge University Press: Cambridge, U.K., 1995.

- (10) Pethig, R. *Crit. Rev. Biotechnol.* **1996**, *16*, 331–348.
- (11) Fuhr, G.; Zimmermann, U.; Shirley, S. G. In *Electromanipulation of Cells*; Zimmermann, U., Neil, G. A., Eds.; CRC Press: Boca Raton, FL, 1996; pp 259–328.
- (12) Wang, X.-B.; Huang, Y.; Wang, X.; Becker, F. F.; Gascoyne, P. R. C. *Biophys. J.* **1997**, *72*, 1887–1899.
- (13) Harrison, D. J.; Li, P.; Tang, T.; Lee, W. In *Proceedings 2<sup>nd</sup> International Symposium on Miniaturized Total Analysis Systems,  $\mu$ TAS96*, Basel, 19–22 November 1996; Widmer, H. M., Ed. *Anal. Methods Instrum.* **1996**, *82*–84.
- (14) Manz, A.; Effenhauser, C. S.; Burggraf, N.; Harrison, J. D.; Seiler, K.; Fluri, K. J. *Micromech. Microeng.* **1994**, *4*, 257–265.
- (15) Ramsey, J. M.; Jacobson, S. C.; Knapp, M. R. *Nat. Med.* **1995**, *1*, 1093–1095.
- (16) Fu, A. Y.; Spence, C.; Scherer, A.; Arnold, F. H.; Quake, S. R. *Nat. Biotechnol.* **1999**, *17*, 1109–1111.
- (17) Li, P. C. H.; Harrison, D. J. *Anal. Chem.* **1997**, *69*, 1564–1568.
- (18) Sosnowski, R. G.; Tu, G.; Butler, W. F.; O'Connell, J. P.; Heller, M. J. *Proc. Natl. Acad. Sci. U.S.A.* **1997**, *94*, 1119–1123.
- (19) Radtkey, R.; Feng, L.; Muralhida, M.; Duhon, M.; Canter, D.; DiPierro, D.; Fallon, S.; Tu, E.; McElfresh, K.; Nerenberg, M.; and Sosnowski, R. *Nucleic Acids Res.* **2000**, *28*, E17.
- (20) Heller, M. J.; Forster, A. H.; Tu, E. *Electrophoresis* **2000**, *21*, 157–164.
- (21) Westin, L.; Xu, X.; Miller, C.; Wang, L.; Edman, C. F.; Nerenberg, M. *Nat. Biotechnol.* **2000**, *18*, 199–204.
- (22) Markx, G. H.; Huang, Y.; Zhou, X. F.; Pethig, R. *Microbiology* **1994**, *140*, 585–591.
- (23) Cheng, J.; Sheldon, E. L.; Wu, L.; Uribe, A.; Gerrue, L. O.; Carrino, J.; Heller, M. J.; and O'Connell, J. P. *Nat. Biotechnol.* **1998**, *70*, 2321–2326.
- (24) Becker, F. F.; Wang, X.-B.; Huang, Y.; Pethig, R.; Vykoukal, J.; Gascoyne, P. R. C. *Proc. Natl. Acad. Sci. U.S.A.* **1995**, *92*, 860–864.

to particle volume,<sup>9</sup> manipulation of molecules including macromolecules demands the use of micrometer- and submicrometer-dimension electrodes and large voltages for producing sufficiently large DEP forces. Thus, little work has been reported in the use of DEP for manipulating molecules.

The combined use of ac and dc fields, however, can complement the limitations of EP and DEP and potentially provides an integrated method for manipulating and separating not only biological cells but also macromolecules. For example, in a sequential fashion, DEP was first used to isolate *Escherichia coli* bacteria on a microchip from whole blood, followed by electronic lysis of the isolated *E. coli* to release the genomic DNA/RNA; and EP was then used to enhance hybridization of the released DNA/RNA on a separate microchip.<sup>23</sup>

In this work, we further explore the use of ac and dc electric fields for manipulation of bioparticles and macromolecules on microfabricated chips. On a microchip scale, DEP is shown to separate *Bacillus globigii* spores and *E. coli* bacteria to different locations. Furthermore, DEP enrichment in a flow cell of microliter volumes is shown for concentrating *E. coli* from a diluted sample and peripheral blood mononuclear cells (PBMNC) from diluted whole blood. Two immune detection methods using dc as well as ac fields are developed for identifying *B. globigii* spores and *E. coli* bacteria with pathogen-specific antibodies.

## THEORY

When a spherical particle of radius  $r$  is subjected to an applied field that comprises both dc and ac components, given by

$$\vec{E} = \vec{E}_{dc} + \vec{E}_{ac} \quad (1)$$

the total electrical forces acting on the particle can be written as

$$\vec{F} = q\vec{E}_{dc} + 2\pi r^3 \epsilon_m \text{Re}(f_{CM}) \nabla E_{rms}^2 \quad (2)$$

where the first term corresponds to the EP component,  $q$  is the effective net charge of the particle, and  $\vec{E}_{dc}$  is the dc field strength at the particle location. The second term is the DEP component,<sup>9,10,27</sup>  $\epsilon_m$  is the absolute permittivity of the suspending medium,  $E_{rms}$  is the rms value of the ac field at the particle location, and  $\nabla$  is the del vector operator. The DEP component is dependent on the interaction between the field nonuniformity factor ( $\nabla E_{rms}^2$ ) and the polarization charge, which is closely associated with the polarization factor  $f_{CM}$ , defined as

$$f_{CM} = (\epsilon_p^* - \epsilon_m^*) / (\epsilon_p^* + 2\epsilon_m^*) \quad (3)$$

In eq 3,  $\epsilon_p^*$  and  $\epsilon_m^*$  are the complex permittivities of the particle and medium, respectively, where  $\epsilon^* = \epsilon - j\sigma/\omega$  and  $\epsilon$  is the permittivity,  $\sigma$  is the conductivity,  $\omega$  is the angular frequency of the applied ac field, and  $j = (-1)^{1/2}$ . The parameter  $\text{Re}(f_{CM})$  is

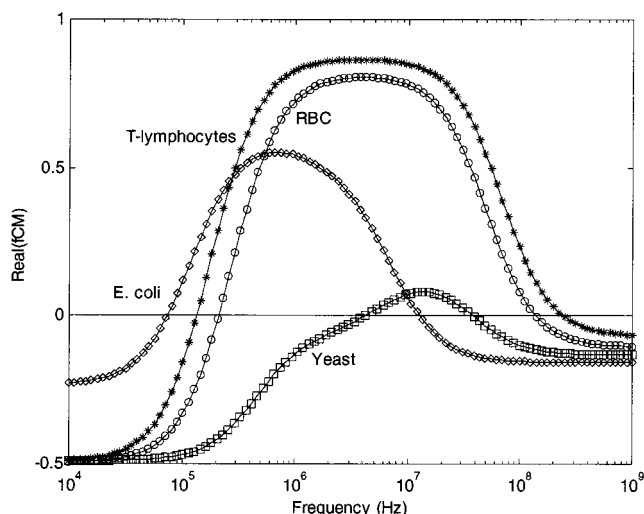


Figure 1. Theoretical frequency spectra for the polarization factor  $\text{Re}(f_{CM})$  for yeast cells ( $\square$ ), heat-killed *E. coli* bacteria ( $\diamond$ ), human erythrocytes ( $\circ$ ), and T-lymphocytes ( $*$ ) simulated according to eq 2, which was based on the dielectric properties of these cells reported earlier.<sup>24,29–31</sup> The electrical conductivity values of the cell suspension medium used in the simulation corresponded to those used in the experiments and were 1200, 20, 235, and 235  $\mu\text{S}/\text{cm}$  for yeast cells, *E. coli* bacteria, human erythrocytes, and T-lymphocytes, respectively.

the real part of the polarization factor  $f_{CM}$ . In a nonuniform field of a given frequency, the cells with positive (or negative)  $\text{Re}(f_{CM})$  experience positive (or negative) DEP forces and are driven toward strong (or weak) electric field regions.<sup>9,10,27</sup>

Equations 2 and 3 show that particles having different dielectric properties (defined by  $\epsilon_p^*$ ) will exhibit different values for the factor  $\text{Re}(f_{CM})$  and experience different DEP forces that may be exploited for particle selective manipulations. Using dielectric shell models<sup>28</sup> for the cells and average dielectric parameters reported previously for yeast cells,<sup>29</sup> *E. coli* bacteria,<sup>30</sup> human erythrocytes,<sup>24</sup> and T-lymphocytes<sup>24,31</sup> (a major subpopulation of peripheral blood mononuclear cells, PBMNC), we calculated the frequency dependencies of the factor  $\text{Re}(f_{CM})$  for the cells suspended in solutions having specific electric conductivities used in this study (Figure 1). Based on such calculations, the separation conditions (e.g., frequency of the applied field) were chosen so that the differences in the  $\text{Re}(f_{CM})$  values between two cell types were maximized. For example, the enrichment of PBMNCs from the mixture with erythrocytes was performed (shown later in Figure 5) at 200 kHz. At this frequency, the difference in  $\text{Re}(f_{CM})$  values between erythrocytes and T-lymphocytes was close to the theoretical maximum. At 200 kHz,  $\text{Re}(f_{CM})$  values for T-lymphocytes and other PBMNCs (their simulated DEP spectra are not shown here) were positive while that for erythrocytes was slightly negative. Thus, PBMNCs were expected to exhibit positive DEP and thus be retained on the electrodes in the presence of a fluid flow. Simultaneously, erythrocytes should exhibit negative DEP and be repelled from the electrodes and, thus, be carried away

(25) Wang, X.-B.; Yang, J.; Huang, Y.; Vykoukal, J.; Becker, F. F.; Gascoyne, P. R. C. *Anal. Chem.* **2000**, *72*, 832–839.

(26) Huang, Y.; Yang, J.; Wang, X.-B.; Becker, F. F.; Gascoyne, P. R. C. *J. Hematother. Stem Cell Res.* **1999**, *8*, 481–490.

(27) Wang, X.-B.; Hughes, M. P.; Huang, Y.; Becker, F. F.; Gascoyne, P. R. C.; *Biochim. Biophys. Acta* **1995**, *1243*, 185–194.

(28) Fuhr, G.; Rosch, P.; Muller, T.; Dressler, V.; Goring, H. *Plant Cell Physiol.* **1990**, *31*, 975–982.

(29) Huang, Y.; Hölzel, R.; Pethig, R.; Wang, X.-B. *Phys. Med. Biol.* **1992**, *37*, 1499–1517.

(30) Hölzel, R. *Biochim. Biophys. Acta* **1999**, *1450*, 53–60.

(31) Yang, J.; Huang, Y.; Wang, X.; Wang, X.-B.; Becker, F. F.; Gascoyne, P. R. C. *Biophys. J.* **1999**, *76*, 3307–3314.



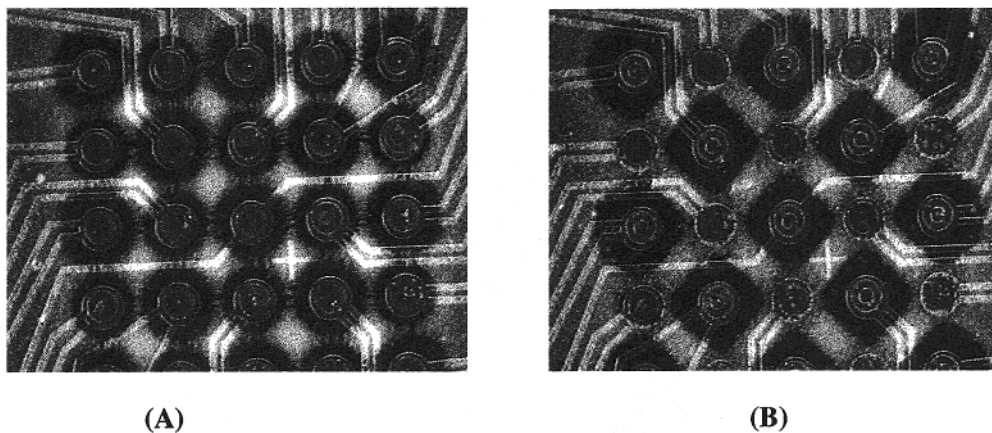


Figure 2. Collection patterns of *S. cerevisiae* yeast cells on the  $5 \times 5$  array with an applied ac voltage at 10 kHz and 8 V(p-p) (A) without and (B) with 1-V dc voltage offset. The yeast cells were suspended in a 50 mM histidine + PBS solution having an electrical conductivity of 1200  $\mu\text{S}/\text{cm}$ .

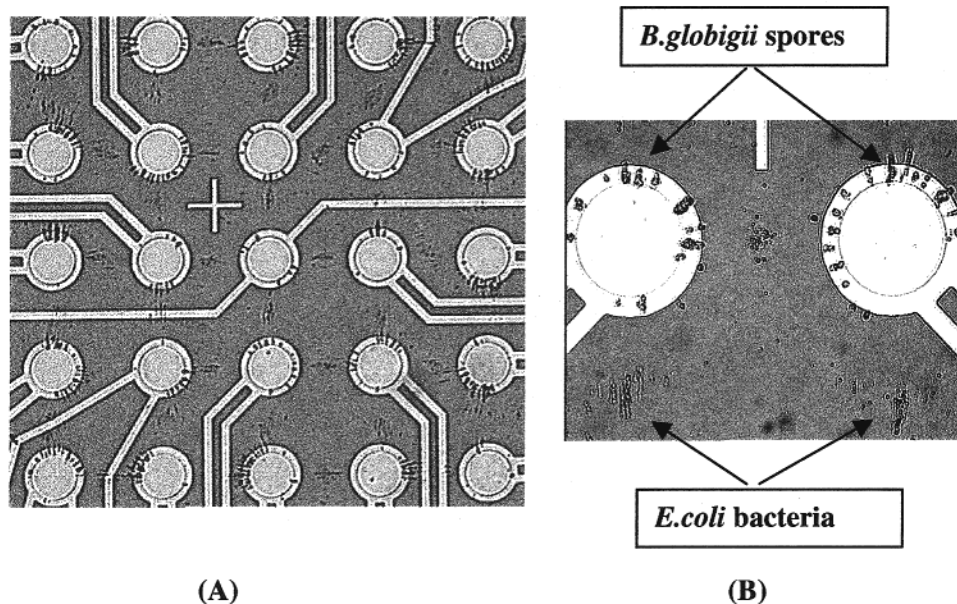


Figure 3. (A) Images representing the microscale separation of *B. globigii* spores and heat-killed *E. coli* bacteria on the  $5 \times 5$  array. The electrodes in the array were addressed with an ac voltage at 50 kHz and 5 V(p-p). The spores and bacteria were suspended in a 280 mM mannitol solution having a conductivity of 20  $\mu\text{S}/\text{cm}$ . (B) Expanded view showing that the spores were collected on the electrodes and the bacteria were repelled from the electrodes.

with the fluid flow. The frequency spectra shown in Figure 1 were based on average cell dielectric parameters. It should be noted that  $\text{Re}(\epsilon_{\text{CM}})$  values for individual cells may be different from theoretical results because of the heterogeneous nature within a cell population.<sup>31</sup>

## EXPERIMENTAL SECTION

**Electrode Fabrication and Cartridge Assembly.** The two electrically active chips (shown in Figures 2 and 4) were designated as the “ $5 \times 5$  array” and “ $\mu\text{-DEP}$ ” chips and were fabricated on silicon wafer using semiconductor processing techniques as described previously.<sup>23</sup> The  $5 \times 5$  array chip consisted of 25 circular, platinum electrodes that were 80  $\mu\text{m}$  in diameter on a 200- $\mu\text{m}$  center-to-center spacing and covered an area of  $0.88 \times 0.88 \text{ mm}^2$ . Other areas on the chip were used for the connection pads to external signal sources and for electric

wires between the  $5 \times 5$  array to these pads. A 1- $\mu\text{m}$  agarose permeation layer that contained streptavidin was prepared on the  $5 \times 5$  array chip using the method described previously.<sup>20</sup> The  $\mu\text{-DEP}$  chip consisted of repetitive sinusoidal-shaped electrodes with a 3- $\mu\text{m}$  tip-to-tip distance and covered an area of  $5 \times 5 \text{ mm}^2$ . There was no permeation layer on the  $\mu\text{-DEP}$  chip.

The chip cartridge was formed by wire binding of the chip to a printed circuit board and was assembled with a flow cell. A polycarbonate molded flow cell and a cover slip were attached to the chip with a UV-cured adhesive to form a sealed chamber. The flow cell was built over an area of  $4.10 \times 4.10 \text{ mm}^2$  covering the electrode-containing area of the chip and had  $\sim 7.5\text{-}\mu\text{L}$  volume with a thickness of 450  $\mu\text{m}$ . Input and output fluidic adapters were formed by plastic tubing with a Luer fitting that were inserted and sealed into the flow cell. A peristaltic pump (model RP-1, Rainin Instruments, Woburn, MA) was connected to either input

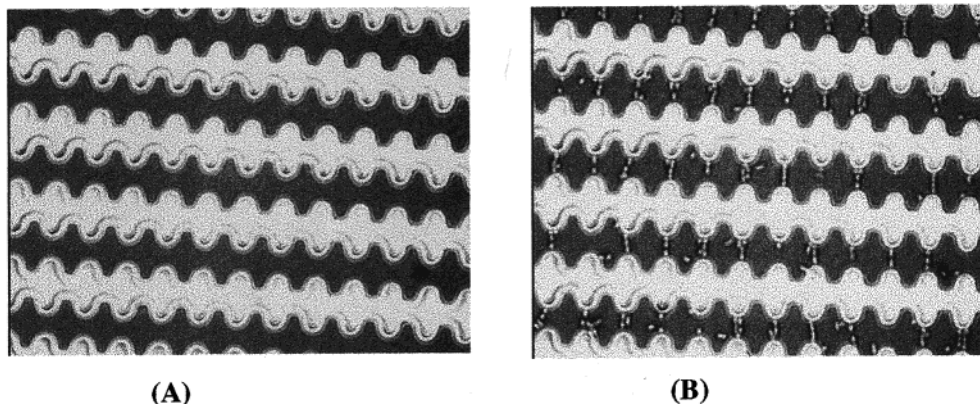


Figure 4. Images showing the enrichment of *E. coli* by flowing the *E. coli* sample, diluted in the deionized water with a conductivity less than  $5\ \mu\text{S}/\text{cm}$ , over the  $\mu$ -DEP chip with an ac voltage at 100 kHz and 3 V(p-p) applied to the electrodes. (A). One area of the electrodes at the beginning of the experiment. (B). The same area at 10 min after the flow started.

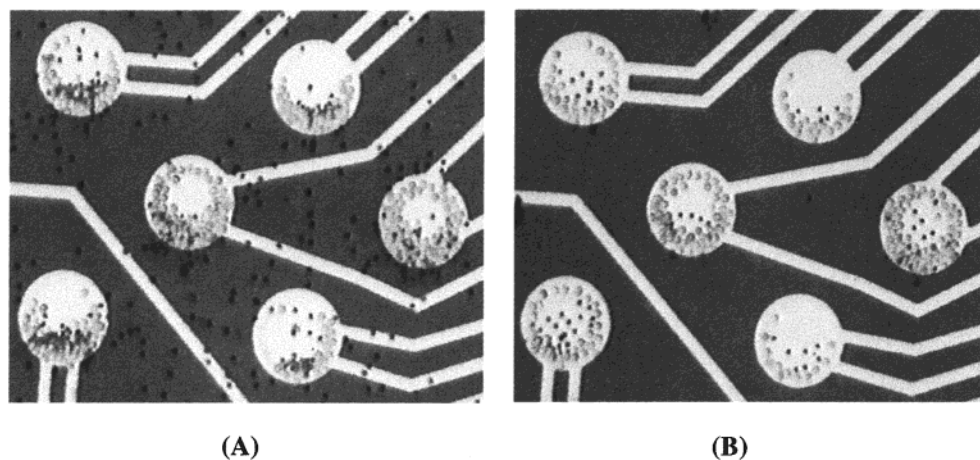


Figure 5. Enrichment of PBMCs from the mixture with RBCs. The data were obtained by flowing the sample at  $\sim 30\ \mu\text{L}/\text{min}$  over a  $5 \times 5$  array with an ac voltage at 200 kHz and 6 V(p-p) applied to the electrodes. The original mixture concentration is  $\sim 1.6 \times 10^7$  cells/mL with the ratio of 1:7 for PBMC/RBC. The conductivity of the sucrose buffer was  $235\ \mu\text{S}/\text{cm}$ . (A) The process of flowing the sample over the chip. (B) The final distribution of cells.

or output tubing of the cartridge for sample introduction and washing protocols. All experiments except the immunoassay for *E. coli* were performed on chips with flow cells.

**Instrumentation.** The electronic connections for the cartridge were accomplished through a home-built switch box that addressed electrical signals to individual electrodes. The ac signals were provided by a signal generator (model HP33120A, Hewlett-Packard, Santa Clara, CA). The dc current was supplied by a Keithley 236 source measurement unit (Keithley Instruments, Cleveland, OH) through a complementary metal oxide semiconductor (CMOS) switch multiplexer.

All images, except those for the immunoassays, were collected through a confocal microscope (Leica INM 100, Leica, Deerfield, IL). The immunoassays for *B. globigii* spores and *E. coli* bacteria were performed on an analytical probe station (model 6000 micromanipulator, Carson City, NV). Fluorescence analysis of Texas Red (TR)-labeled antibodies in the spore assay was provided by two 594-nm HeNe lasers (6-mW output power; Research Electro-Optics, Boulder, CO) that illuminated the field of interest through optical fibers (1 mm in diameter) at an oblique angle. Fluorescence was collected through an  $8\times$  objective lens (numerical aperture 0.15) and passed through a narrow band-pass filter (20 nm) centered at 620 nm.

The fluorescence analysis in the *E. coli* assay was conducted by selecting the appropriate filter set for TR or fluorescein (FL) where necessary. Optical analysis was performed by epifluorescence on a Leica DMLM epifluorescent microscope ( $10\times$  objective lens) with a tungsten lamp as the excitation source. Excitation and fluorescence collection were accomplished with the appropriate narrow band-pass filter set, specifically designed for either fluorescein (Ex 480/30, Em 535/40) or Texas Red (Ex 582/30, Em 632/50) fluorophores.

Fluorescence images in all cases were taken by a cooled CCD camera (model TEA/CCD-512-2KB1, Princeton Instruments, Trenton, NJ). All image acquisition and data analysis were achieved by means of a color frame grabber (Scion, Frederick, MD) and the IP Lab spectrum software (Signal Analytics Corp., Vienna, VA) on a Macintosh Power PC 7300/180.

**Bioparticle Preparations.** *B. globigii* spores (the Biological Defense Research Directorate, Bethesda, MD) were stocked in phosphate-buffered saline (PBS, pH 7.2; Life Technologies, Grand Island, NY) at a concentration of  $1.4 \times 10^9$  spores/mL. Heat-killed *E. coli* O157:H7 bacteria (KPL, Gaithersburg, MD) were stocked in distilled water at a concentration of  $7 \times 10^9$  bacteria/mL. *Saccharomyces cerevisiae* baker's yeast (type I, Catalog No. YSC-1; Sigma, St. Louis, MO) were rehydrated and stocked in PBS at



Table 1. SDA Primers for *E. coli* SLT-1 Gene

ID	function	sequence (5'–3')
2725	primer	TTATATGTGGCAGGATTTGTTCTCGGGACAAATAATG
2727	primer	AGCTACTGTCAACGACAATGCTCGGGCTGTTGTACCT
2726	primer bumper	ACGGCTTATTGTTGAACGAA
2728	primer bumper	CTGCAACACGCTGTAACGTG

the concentration of 10 mg/mL. In the yeast manipulation experiment,  $5 \times 10^9$  yeast were washed 2 times and resuspended in 1 mL of 50 mM histidine having a conductivity of 1200  $\mu\text{S}/\text{cm}$  adjusted by adding PBS buffer.

PBMNC (San Diego Blood Bank, San Diego, CA), isolated by gradient centrifugation,<sup>32</sup> were mixed with red blood cells (RBC) at a ratio of 1:7 in a DEP buffer (250 mM sucrose, 2.5  $\mu\text{M}$  Tris, 2.5  $\mu\text{M}$  boric acid, 0.05  $\mu\text{M}$  EDTA, pH 8.2). The final cell suspension conductivity and concentration were 235  $\mu\text{S}/\text{cm}$  and  $1.6 \times 10^7$  cells/mL, respectively.

**Bioparticle Separation.** Heat-killed *E. coli* bacteria and *B. globigii* spores were washed 3 times in 280 mM mannitol (Sigma) and resuspended in the mannitol solution having a conductivity of 20  $\mu\text{S}/\text{cm}$ . The final mixture concentration was  $2 \times 10^8/\text{mL}$  and  $3 \times 10^8/\text{mL}$  for bacteria and spores, respectively. Microscale separation was achieved by applying an ac voltage at 50 kHz, 5 V(p–p) to the  $5 \times 5$  array, in which adjacent electrodes along either horizontal or vertical lines were applied with signals of the opposite polarity. This method of addressing will be referred to as “checkerboard” mode.

**Bioparticle Enrichment.** In the *E. coli* experiment, 5 mL of diluted *E. coli* suspension in deionized water was continuously pumped through the flow cell that contained the  $\mu\text{-DEP}$  chip at 400  $\mu\text{L}/\text{min}$  while a 100-kHz, 3-V(p–p) voltage was applied to the chip. The DEP-collected *E. coli* bacteria were eluted from the chip by flushing the chip with deionized water at 400  $\mu\text{L}/\text{min}$  for 30 s after the ac voltage was turned off. The collected samples were counted for cell concentrations or stored at  $-20^\circ\text{C}$  for further analysis.

In the PBMNC enrichment experiment, the PBMNC and RBC mixture in the DEP buffer described above in Bioparticle Preparations was continuously transported through the flow cell that contained a  $5 \times 5$  array chip at 30  $\mu\text{L}/\text{min}$  for 30 min. Simultaneously, the electrodes on the chip were addressed by an ac voltage of 200 kHz, 6 V(p–p) in the checkerboard mode. Afterward, the chip was washed with the DEP buffer at 30  $\mu\text{L}/\text{min}$  for 10 min and at 60  $\mu\text{L}/\text{min}$  for an additional 10 min with the voltage on. Finally, the number of PBMNC and RBC remaining on each electrode was counted manually by microscopy.

**SDA Amplification.** A strand displacement amplification (SDA) protocol<sup>21</sup> was optimized to detect the *E. coli* SLT-1 gene. Deoxynucleoside 5'-triphosphates (dGTP, dATP, dTTP) and MgOAc were purchased from Pharmacia (Alameda, CA). 2'-Deoxycytosine 5'-O-(1-thiophosphate) (dCTP $\alpha$ S), BsoB1 restriction endonuclease, and Bst polymerase were supplied by Becton Dickinson (Sparks, MD). Oligonucleotides (primers and primer bumpers) were synthesized by Synthetic Genetics (San Diego, CA) and are shown in Table 1. Each reaction contained 5  $\mu\text{L}$  of

*E. coli* bacteria suspension and 35  $\mu\text{L}$  of SDA mixture (35 mM  $\text{KHPO}_4$ , 1.4 mM each dCTP $\alpha$ S, dTTP, dATP, and dGTP, 9.75 mM MgOAc, 80  $\mu\text{g}/\text{mL}$  BSA, 500 nM SDA primer, and 50 nM primer bumper). The 40- $\mu\text{L}$  solution was first incubated at  $95^\circ\text{C}$  for 5 min to denature bacteria and was then incubated at  $60^\circ\text{C}$  for 2 min followed by addition of 10  $\mu\text{L}$  of enzyme mixture (17.5 mM  $\text{KHPO}_4$ , 40  $\mu\text{g}/\text{mL}$  BSA, 1.76 units/reaction BsoB1, and 3.78 units/reaction BstI polymerase) into each reaction. The SDA reaction was executed at  $60^\circ\text{C}$  for 30 min. The SDA products were checked by electrophoresis on a 10% TBE polyacrylamide gel (Novex, San Diego, CA).

**Immunoassay for *B. globigii* and *E. coli*.** The assay was performed on  $5 \times 5$  array chips in 50 mM histidine buffer. For the *B. globigii* assay, polyclonal goat anti-*B. globigii* antibody (Biological Defense Research Directorate) and polyclonal rabbit anti-malathion antibody (Fitzgerald Industries International, Concord, MA) were labeled in-house with TR-x-succinimidyl ester (Molecular Probes, Eugene, OR) and used as the detecting antibodies. For the *E. coli* assay, monoclonal anti-*E. coli* antibody (ViroStat, Portland, ME), monoclonal anti-cholera toxin B (CTB) antibody (Karlan Research Products Corp., Santa Rosa, CA), and monoclonal anti-staphylococcal enterotoxin B (SEB) antibody (the Biological Defense Research Directorate) were labeled with biotinyl-xx-succinimidyl ester and TR-x-succinimidyl ester to serve as capture antibodies. Fluorescein (FL)-labeled goat anti-*E. coli* O157:H7 F(ab')<sub>2</sub> antibody fragments (KPL) were used as detecting antibody. Protein toxin, SEB (Sigma), labeled in-house with fluorescein (FL-SEB, Sigma), and fluorescein-labeled CTB (FL-CTB, Sigma) were used as spikes in the *E. coli* assay. All the listed antibodies were dialyzed against 50 mM histidine buffer (conductivity of 62  $\mu\text{S}/\text{cm}$ ) before use.

A direct immunoassay was used for *B. globigii* spores, which consisted of two steps of dc current application: collecting *B. globigii* spores on the electrodes and addressing the detecting antibodies to the electrodes. The surface of the flow cell was blocked by 0.1% BSA in PBS/Tween 20 overnight at  $4^\circ\text{C}$  prior to experiments. For the assay,  $4 \times 10^7$  spores in 40  $\mu\text{L}$  of 50 mM histidine, having a conductivity of 266  $\mu\text{S}/\text{cm}$ , were first introduced into the flow cell through the inlet by a peristaltic pump. Spores were then collected continuously by electrophoresis onto 12 positively biased electrodes at an applied dc current of 100 nA/electrode (the dc potential was 2.4 V) for total of 6 min. In the time segment between 1.5 and 3.5 min after the dc current was applied, the flow cell and inlet tubing were washed by reverse flowing 50 mM histidine for 2 min at 45  $\mu\text{L}/\text{min}$  in the continued presence of the dc current. After the spore collections, TR-labeled polyclonal goat anti-*B. globigii* antibody, diluted in 50 mM histidine/0.1% Tween 20 to a final concentration of 3.1  $\mu\text{g}/\text{mL}$ , was then introduced into the flow cell through the inlet at 45  $\mu\text{L}/$

(32) Boyum, A. *Scand. J. Clin. Lab. Invest.* **1968**, 21 (Suppl. 97), 77–89.

min for 1 min. The antibodies were then addressed continuously by electrophoresis to 16 positively biased electrodes at an applied dc current of 125 nA (the dc potential was 2.5 V) for 1 min. The dc current was then turned off and the flow cell was washed by reverse flowing histidine from the buffer reservoir for 4 min at 45  $\mu\text{L}/\text{min}$  to wash off any unbound antibodies. The assay process was visualized under white light and fluorescence microscopes.

A sandwich-format immunoassay was used for detecting *E. coli* bacteria. This assay format included three steps: (1) immobilizing capture antibodies on electrodes with a dc current; (2) collecting *E. coli* to these electrodes with an ac voltage; (3) addressing FL-labeled detecting antibodies with a dc current. A 10- $\mu\text{L}$  aliquot of biotinylated TR-labeled monoclonal anti-*E. coli* capture antibody (5  $\mu\text{g}/\text{mL}$ ) was first micropipetted onto the chip. The antibodies were then addressed by electrophoresis to the selected, positively biased electrodes at an applied dc current of 400 nA/electrode for 2 min with a 10-s current-off segment in the middle. The chip was then washed by pipetting with excess 50 mM histidine to remove unbound capture antibodies. Next, a 10- $\mu\text{L}$  volume of heat-killed *E. coli* bacteria ( $10^8/\text{mL}$ ) or 10  $\mu\text{L}$  of mixture of *E. coli* ( $10^8/\text{mL}$ ) with FL-SEB (240  $\mu\text{g}/\text{mL}$ ) and FL-CTB (240  $\mu\text{g}/\text{mL}$ ) was added by pipetting onto the chip that was loaded with capture antibodies on selected electrodes. *E. coli* bacteria were then collected on the selected electrodes by applying an ac voltage of 5 kHz, 5 V(p-p) for 5 min to the electrodes. The chip was then washed extensively with 50 mM histidine buffer by pipet. To detect the presence of *E. coli* bacteria, 10  $\mu\text{L}$  of FL-labeled polyclonal goat anti-*E. coli* detecting antibody (10  $\mu\text{g}/\text{mL}$ ) was micropipetted onto the chip and consequently addressed onto the corresponding electrodes (used as anode) at a dc current of 200 nA/electrode for 1 min. The chip was extensively washed again with 50 mM histidine buffer to remove unbound detecting antibodies. The images were taken under the white light and fluorescence microscopes.

## RESULTS AND DISCUSSION

### Manipulation of Yeast Cells Using ac and ac/dc Fields.

Figure 2A demonstrates a typical collection pattern of yeast cells that results from DEP under the influence of an ac electrical voltage at 10 kHz, 8 V(p-p). At such low frequencies of the applied field, the yeast cells were less polarizable than the suspending medium because of their poorly conducting plasma membrane and, thus, exhibited negative DEP (see the DEP frequency spectrum of yeast cells in Figure 1).<sup>29</sup> In this instance, cells were repelled from the electrodes and were collected in the weak-field regions at the interelectrode spaces. Figure 2B shows the cell distribution after a 1-V dc voltage was superimposed to the previous 8-V ac voltage. In this case, the cells were subjected to EP forces that drove the cells toward the negatively biased electrodes and previously applied negative DEP forces that drove the cells toward the interelectrode spaces. Thus, the cells were collected at the edges of the negatively biased electrodes and formed bands between those electrodes. It is important to note that yeast cells in the histidine buffer used in this study exhibited net, positive charges as verified in a separate EP experiment where the cells were observed to move toward negatively biased electrodes. The results in Figure 2 show that variation of applied field conditions could lead to flexible manipulation of particles.

### Microscale Separation of *B. globigii* Spores from *E. coli*

**Bacteria.** Figure 3A shows the distribution of *B. globigii* spores and heat-killed *E. coli* O157:H7 bacteria on a  $5 \times 5$  chip after an ac voltage at 50-kHz, 5-V(p-p) field was applied for 2 min. The expended view in Figure 3B revealed that the spores were collected on the electrodes under positive DEP forces whereas the bacteria were repelled from those electrodes by negative DEP forces. The differential DEP responses between the spores and *E. coli* arose from the structural and compositional differences between these particles. At 50 kHz, the poorly conducting plasma membrane of the bacteria dominated their dielectrophoretic behavior, and the bacteria were less polarizable than the surrounding medium (conductivity 20 mS/cm) and exhibited negative DEP (see the frequency spectrum for the bacteria in Figure 1). Even though the spores (~1  $\mu\text{m}$  in diameter) are also composed of a poorly conducting plasma membrane, their relatively conducting cortex and coat layers<sup>33</sup> determined that the spores were more polarizable than the surrounding medium and exhibited positive DEP. This result demonstrates that two types of particles having different structural and compositional differences can exhibit different DEP characteristics and can thereby be selectively manipulated. It is worthwhile to note that the heat-killed *E. coli* bacteria exhibited little or no DEP effects when they were suspended in solutions of moderate or high conductivities (>50  $\mu\text{S}/\text{cm}$ ). Thus, to achieve appreciable DEP effects for the heat-killed *E. coli*, the suspension conductivity was chosen to be a very low value of 20  $\mu\text{S}/\text{cm}$ .

The microscale separation described here exploited the opposite DEP forces exerted on the two types of bioparticles under appropriate separation conditions (e.g., the frequency of the applied field, the electrical conductivity of the solution). The performance of such separations is dependent on the dielectric properties of the bioparticles to be selectively manipulated. Wide distribution in bioparticle dielectric properties may result in individual bioparticles of the same type exhibiting opposite DEP effects, leading to a noncomplete separation of the bioparticles on the chip. With known dielectric properties and their distributions for the bioparticles, it is possible to analyze the separation performance. Because the dielectric properties of *B. globigii* spores were unknown at the time, such theoretical analysis was not performed and the applied field frequency for the separation was empirically discovered.

**Enrichment of *E. coli* Bacteria.** An important application of chip-based bioparticle manipulation is the capability to concentrate bioparticles from samples so that relatively low copy numbers may be analyzed. To demonstrate this, a dielectrophoretic enrichment of *E. coli* bacteria from a diluted sample was performed on a  $\mu\text{-DEP}$  chip. The samples were pumped through the  $\mu\text{-DEP}$  chip-based flow cell with appropriate ac signals being applied to the electrodes so that *E. coli* bacteria were continuously collected to the electrodes by positive DEP forces. Panels A and B of Figure 4 show an area of the chip at the beginning of the experiment and at 10 min after the flow was started, respectively. The cell count for the original and enriched samples on a hemacytometer revealed that a 20-fold enrichment was achieved as the *E. coli* concentration increased from  $2 \times 10^3/\mu\text{L}$  to  $4 \times 10^4/\mu\text{L}$ . From these results, it is of interest to determine the bioparticle collection

(33) Stragier, P.; Losick, R. *Annu. Rev. Genet.* **1996**, *30*, 297–341.

efficiency under such conditions. A 5-mL sample at a concentration of  $2 \times 10^3/\mu\text{L}$  was pumped through the flow cell that contained a total of  $10^7$  bacteria. The final eluted sample of  $200 \mu\text{L}$  at  $4 \times 10^4/\mu\text{L}$  contained a total of  $8 \times 10^6$  bacteria. Thus, the DEP collection of *E. coli* was  $\sim 80\%$  efficient. This result illustrates that DEP may potentially be used as a powerful means for collecting bioparticles from dilute suspensions.

To further validate the method, diluted *E. coli* samples with concentrations of 8, 20, and 40 bacteria/ $10 \mu\text{L}$  were enriched on the  $\mu$ -DEP chip under similar DEP and flow conditions. The DEP-collected bacteria were eluted from the flow cell by washing the chip with deionized water, and they were collected in  $100\text{-}\mu\text{L}$  aliquots for SDA analysis of *E. coli* SLT-1 gene. For each  $45 \mu\text{L}$  of SDA reaction volume, an additional  $5 \mu\text{L}$  of corresponding sample was introduced as the template. The SDA products were examined on a 10% TBE gel (data not shown). For the three tested concentrations, the DEP-enriched samples yielded gel bands of greater intensity than the corresponding preload samples. Thus, the application of a DEP field on the  $\mu$ -DEP chip was qualitatively effective in enriching *E. coli* even at these low concentrations and adequate amounts for genetic analysis could be recovered.

**Enrichment of PBMNCs from RBCs.** By competing the fluidic force with the DEP force exerted on cells, enrichment of one type of cells from a cell mixture could be achieved. This was demonstrated in a study where a mixture of PBMNCs and RBCs was made to flow over a  $5 \times 5$  array chip with ac electrical signals being applied to the electrodes. Under appropriate DEP and fluid-flow conditions, PBMNCs were selectively collected onto the electrodes and trapped there in the presence of the flow stream. Simultaneously, RBCs were carried away by the fluid flow (Figure 5A). The final cell distribution on the chip is shown in Figure 5B. The on-chip cell count revealed that, after the enrichment, the PBMNC to RBC ratio increased from 1:7 to 4:1. To demonstrate this method further, freshly drawn whole blood was subjected to the same enrichment procedure. In this case, the whole blood was diluted by 3500-fold in the DEP buffer to reach a cell concentration of  $1.5 \times 10^6$  cells/mL with a WBC/RBC ratio of 1:1000 and conductivity of  $230 \mu\text{S}/\text{cm}$ . For this sample, the DEP collection on the chip also resulted in an enrichment of  $\sim 30$ -fold for WBCs. This result is comparable with the reported DEP field-flow-fractionation studies for similar cell separation problems.<sup>26</sup>

34

The DEP field frequency for enriching PBMNCs in this work was chosen from the simulated frequency spectra for the cells (Figure 1) in order to maximize the differences between DEP forces exerted on PBMNCs and RBCs, as described in the Theory section. The fluid flow rate in the study was empirically chosen through visual determination for maximizing and minimizing collection of PBMNCs and RBCs, respectively. Like the microscale on-chip separation of cells, the performance of such DEP enrichment depends on the dielectric properties of the cells to be separated. By knowing the cell dielectric properties and their distributions, the field distribution, and the fluid-flow profile in the DEP-chip containing flow cell, it is possible to predict not only the optimum flow conditions according to the competition<sup>24</sup> between the DEP forces and fluid-flow forces on the cells but also

the enrichment performance in terms of cell enrichment factor and purity.

**Immunoassays.** In the previous examples, the manipulation of bioparticles was demonstrated in several ways. First, the application of DEP and a combination of DEP and EP resulted in the flexible manipulation of particles. On the  $\mu$ -DEP chip, the enrichment of *E. coli* bacteria was shown for an electrode design where the electrode pattern nearly encompassed the entire area of the flow cell. Finally, the DEP separations of *E. coli* and *B. globigii* spores, and PBMNCs and RBCs on a  $5 \times 5$  array chip were successfully performed under static and dynamic fluid-flow conditions. Although DEP has exhibited versatility in these previous examples, this technique does not provide the absolute molecular or bioparticle recognition that is necessary for diagnosing targets from unknown samples or from a sample with several targets. By applying DEP to concentrate and allocate sample to specific locations, these techniques may be further refined to provide enhanced diagnostic applications. Consequently, the remainder of this section will incorporate DEP where both ac and dc fields are utilized to develop electric field-driven immunoassays for detecting *B. globigii* spores and *E. coli* bacteria.

**Spore Immunoassays.** Typical images for a dc field-driven spore immunoassay are shown in Figure 6. The electrode configurations for the  $5 \times 5$  chip are illustrated in Figure 6A, in which the electrodes addressed for spores and for TR-labeled antibodies are represented by "S" and gray color, respectively. Panels B and C of Figure 6 are the images of the spores that were collected on 12 positively biased electrodes, due to the applied dc currents (100 nA/electrode), under white light and laser illuminations, respectively. The spores remained on the selected 12 electrodes after removal of the dc current. Their adhesion to the electrodes is most likely to be due to the inherent sticky nature of proteins that form the thick, outer coating of the spore.<sup>33</sup> Due to their large size ( $\sim 1 \mu\text{m}$ ), they tend to scatter the excitation laser that results in elevated background signals. The images of the  $5 \times 5$  array chip under laser illumination are shown in Figure 6D, after 16 positively biased electrodes were addressed with TR-labeled anti-*B. globigii* spore antibodies by applying a dc current (125 nA/electrode). The effectiveness of the electrically addressing of antibodies over the passive diffusion of antibodies onto the electrodes was evident since the fluorescence levels over the electrodes addressed with both spores and antibodies were significantly greater than the electrodes addressed with only spores but not antibodies. Little nonspecific binding of the detecting antibodies to the electrodes without spores occurred, as indicated by the low light intensity over those electrodes. The total time for performing this assay was less than 15 min.

To further validate the assay, a titration curve and cross-reactivity characteristics of the detecting antibody were determined. At a given spore concentration ( $10^9/\text{mL}$ ) and a fixed electronic condition for addressing spores onto the electrodes, a series of TR-labeled anti-*B. globigii* spore antibody concentrations (at 0.3, 1.0, 3.1, and  $10.3 \mu\text{g}/\text{mL}$ ) were used in the assay for electrically addressing to the spore-loaded electrodes. Comparison of fluorescent intensities between electrodes addressed with TR-labeled antibodies at different concentrations revealed that a concentration of  $3.1 \mu\text{g}/\text{mL}$  for antibodies yielded the greatest fluorescent signals (Figure 6E). To investigate potential cross-

(34) Muller, T.; Schnelle, T.; Gradl, G.; Shirley, S. G.; Fuhr, G. *J. Liq. Chromatogr., Relat. Technol.* **2000**, *23*, 47–59.



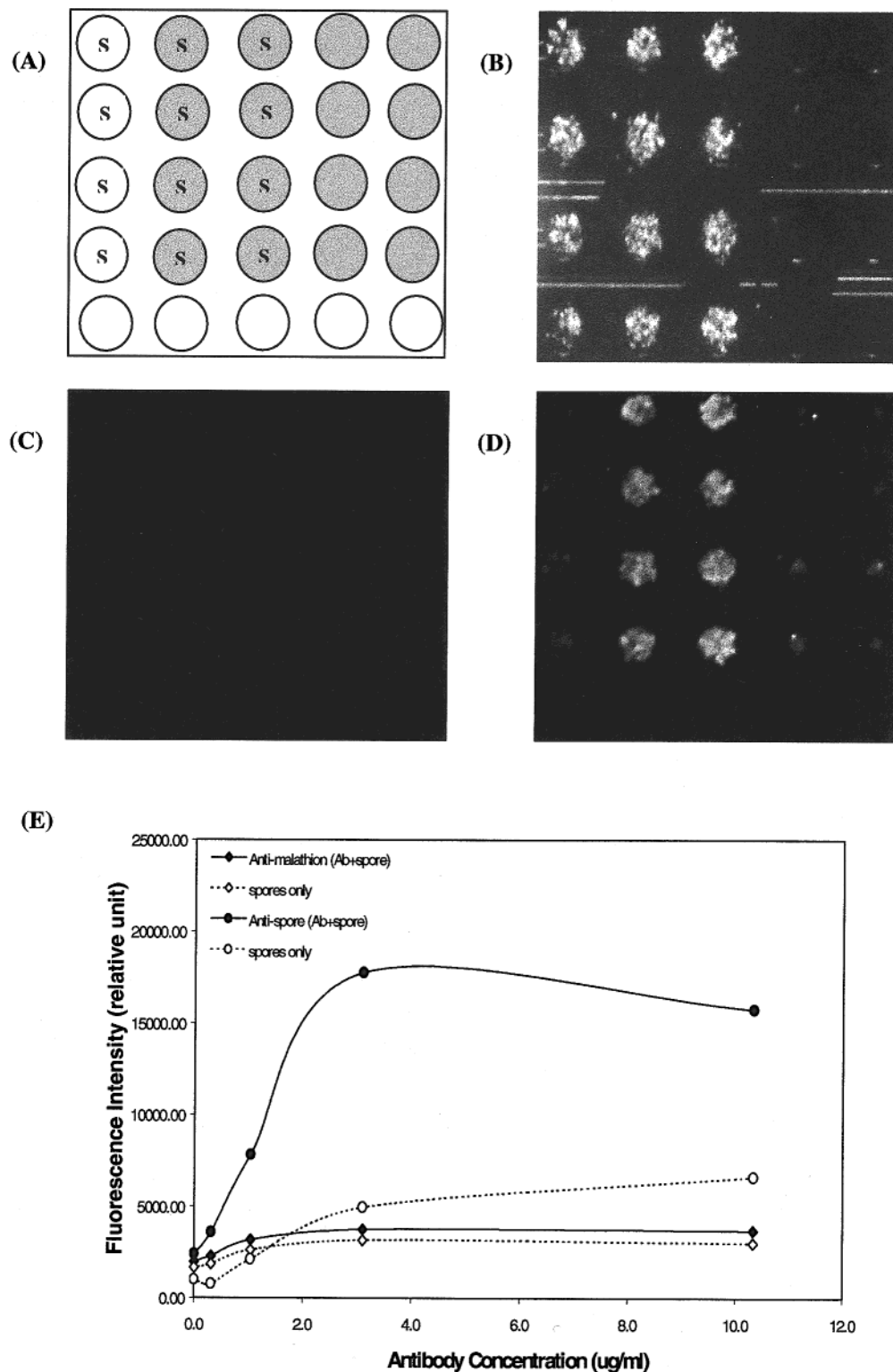


Figure 6. Electric field-mediated two-step immunoassay for *B. globigii* spores. (A) Schematic representation of the addressing configuration is given where spores were addressed to the electrodes (used as anode) marked by "S" at 100 nA/electrode for 6 min. TR-labeled polyclonal goat anti-*B. globigii* antibodies were addressed to the electrodes (used as anode) marked with gray at 125 nA/electrode for 1 min. (B) White light image obtained after the dc electric current was applied for addressing the spores to the electrodes. (C) Fluorescent image after the dc current was applied for addressing the spores to the electrodes. (D) Fluorescent image after TR-labeled polyclonal goat anti-*B. globigii* antibodies were addressed. (E) Titration and specificity for *B. globigii* spore immunoassay.

reactivity between spores and nonspecific antibodies, a similar titration experiment was also performed for TR-labeled polyclonal rabbit anti-malathion antibodies on a separate chip. The fluorescent intensities for anti-malathion antibodies were at the fluorescence

background level and were 4–5 times less than those for anti-spore antibodies.

To quantify the cross-reactivity of spores with nonspecific antibodies (TR-anti-malathion), additional experiments were per-

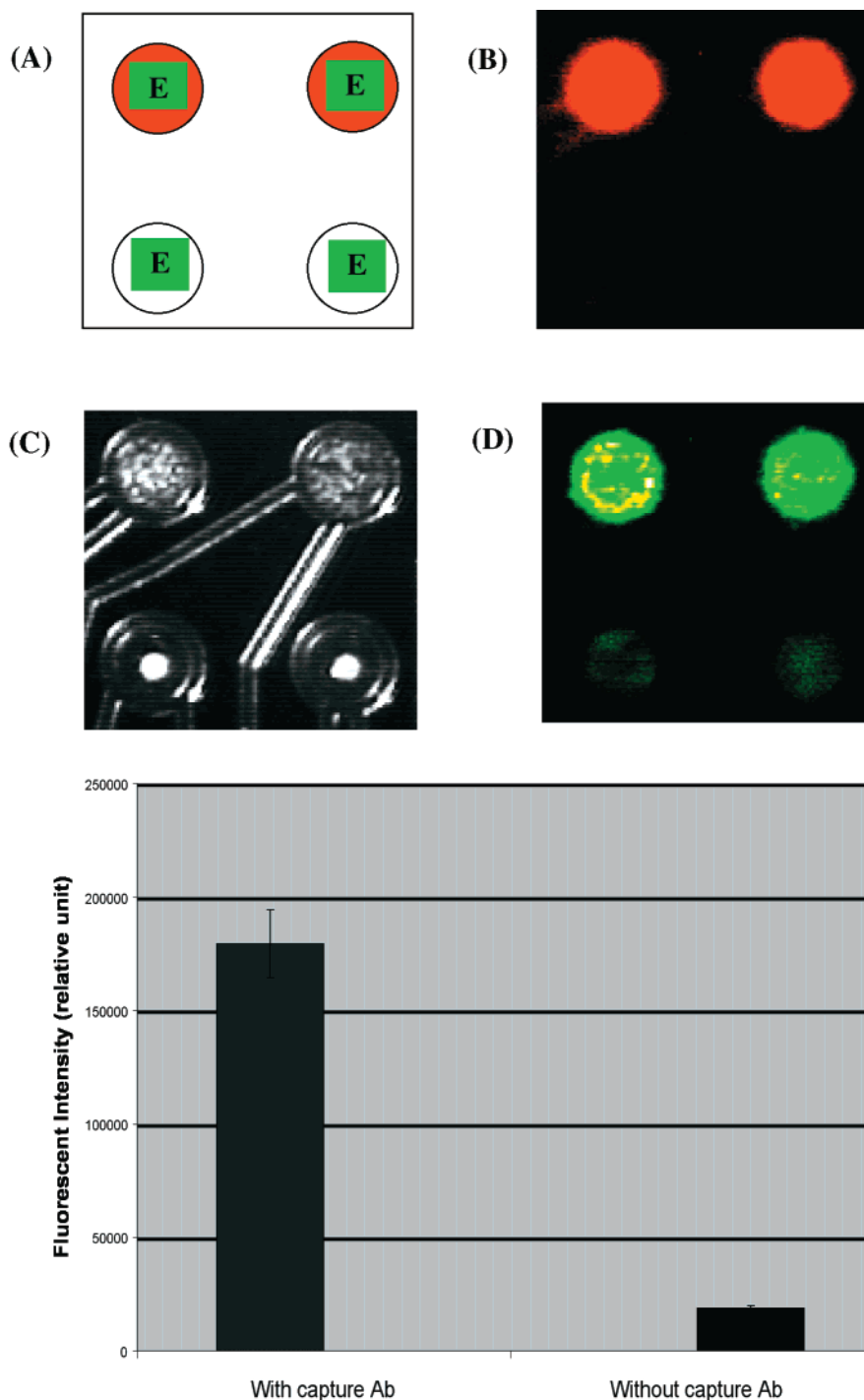


Figure 7. Electric field-mediated three-step immunoassay for *E. coli* bacteria. (A) Schematic representation of the addressing configuration is provided where biotinylated TR-labeled monoclonal anti-*E. coli* antibodies were addressed to the top two electrodes (used as anode, marked with red) at 400 nA/electrode for 2 min. Heat-killed *E. coli* bacteria were addressed to all the four electrodes (marked by letter "E") at 5 kHz, 5 V(p-p) for 5 min. FL-labeled goat anti-*E. coli* O157:H7 F(ab')<sub>2</sub> antibody fragments were addressed to all the four electrodes (used as anode, marked with green) at 200 nA/electrode for 1 min. (B) Fluorescent image after biotinylated TR-labeled monoclonal anti-*E. coli* antibodies were addressed. (C) Light image after heat-killed *E. coli* bacteria was addressed. (D) Final fluorescent image after FL-labeled goat anti-*E. coli* O157:H7 F(ab')<sub>2</sub> antibody fragments was addressed. (E) FL fluorescence intensity on the electrodes with and without capture antibodies.

formed on a single chip to ensure comparable assay conditions. After spores were electrically captured on the electrodes, the anti-spore antibodies were addressed to certain electrodes, followed by a washing process to remove any unbound antibodies. The fluorescence levels were measured on the spore-loaded electrodes with and without addressed antibody. Then the above process was repeated for the anti-malathion antibodies. The binding

efficiency between spores and antibodies was quantified using the fluorescence intensity on the spore-loaded electrodes normalized against the white light intensity of the spores. This normalization took into account the variation of spore numbers on different electrodes. The ratio of the binding efficiency at the electrodes with electrically addressed antibodies to the electrodes without addressed antibodies was 13.7 for the anti-spore antibodies. This

ratio was 4.2 for anti-malathion antibodies, however, indicating that there was some degree of cross-reactivity between the nonspecific antibodies and the spores. The specificity of spore detection in this assay is about 3.3:1. Cross-reactivity between these spores and nonspecific antibodies was also observed in ELISA assays.<sup>36</sup> Compared with classical immunoassays, this dc field-mediated *B. globiggi* immunoassay has the advantages of fast reaction (~15 min) and no need for additional capture antibodies.

***E. coli* Immunoassay.** In above spore immunoassay, the sample contained only target spore particles. For a sample containing multiple bioparticle types, however, separating one target type from the sample for the followup bioassay may provide advantages of reduced cross reactivity and improved signal-to-noise ratio. For example, in the application of analyzing an environmental sample that may contain micrometer-sized bacteria and protein toxins, it may be necessary to first separate the bacteria and protein toxins and then perform assays on purified samples. Such a separation can be achieved by selective DEP collection of bacteria from the mixture sample with an ac field. DEP forces acting on micrometer-sized bacteria can be  $10^6$  times stronger than the forces on protein toxins (assuming a 10-nm dimension). Thus, an appropriately applied ac field configuration can result in the collection of bacteria with no effect on protein toxins. In the following, we shall first demonstrate the feasibility of immunoassay detection of a pure *E. coli* sample by a combined dc and ac field and then show the method can also be applied to an *E. coli* sample spiked with two fluorescein-labeled protein toxins, FL-SEB and FL-CTB.

The dc and ac field-mediated sandwich assay for *E. coli* is shown in Figure 7. The electrode configurations for the  $5 \times 5$  chip are shown in Figure 7A, in which "E" represents the electrodes addressed with *E. coli*, red represents the electrodes with biotinylated TR-labeled anti-*E. coli* capture antibodies, and green represents the electrodes with FL-labeled detecting antibodies. Biotinylated anti-*E. coli* capture antibodies were first loaded on the top row of electrodes by applying dc current and were immobilized on the electrodes through biotin binding to streptavidin in the permeation layer (Figure 7B). *E. coli* bacteria were then addressed to the four electrodes through DEP using ac signals at 5 kHz, 5 V(p-p). It was observed that *E. coli* collection patterns were different between the electrodes with and without the capture antibodies (Figure 7C). For the electrodes with capture antibodies (top row of electrodes), *E. coli* bacteria were dispersed over the entire electrode area. We attribute this phenomenon to the capture of *E. coli* by specific antibodies preimmobilized over the entire electrodes as they were attracted by DEP forces toward the field maximum, located at the center of the electrodes. In the absence of specific capture antibodies on the electrodes (bottom two electrodes), the *E. coli* bacteria were accumulated at the center regions of the electrode (Figure 7C). This observation was confirmed by an additional experiment in which *E. coli* bacteria were also collected at the central regions of the electrodes that had been preimmobilized with nonspecific, anti-SEB or anti-CTB antibodies (data not shown).

After *E. coli* bacteria were collected onto the electrodes, the ac field was turned off and a washing step was employed to remove

the unbound *E. coli*. The bacteria that remained on the electrodes after washing were immune-detected by addressing the FL-labeled anti-*E. coli* detecting antibody to all the four electrodes with a dc current (Figure 7D). The fluorescent intensity on the electrodes with and without capture antibody was measured. According to Figure 7E, the ratio of fluorescent intensity for electrodes with capture antibodies to that for electrodes without capture antibodies was ~9.6.

Using the above protocol, we also performed an electric field-mediated immunoassay for *E. coli* in a mixture with FL-SEB and FL-CTB proteins. After biotinylated TR-labeled monoclonal anti-*E. coli* capture antibodies were loaded onto the electrodes by applying a dc current, an aliquot of the mixture of *E. coli* and FL-SEB and FL-CTB was pipetted onto the chip and an ac voltage was then applied to selected electrodes. It was observed that *E. coli* bacteria were collected on the selected electrodes. Furthermore, the fluorescent intensity on all the electrodes, ac addressed or not, was similar indicating that FL-labeled SEB and CTB proteins were not collected by the field. This is different from previous work,<sup>35</sup> in which both FL-SEB and FL-CTB proteins were transported to and collected at the electrodes under the influence of a dc current. Finally, the uncollected FL-SEB and FL-CTB proteins and unbound *E. coli* were washed with 50 mM histidine buffer, and the collected *E. coli* bacteria were detected by addressing FL-labeled polyclonal goat anti-*E. coli* detecting antibodies via a dc field. In this assay for detecting *E. coli* from a mixture, the ratio of fluorescent intensity for electrodes with capture antibodies to electrodes without capture antibodies was ~6.2, which is a similar value achieved for detecting the pure *E. coli* sample described above.

This is the first time where combined use of EP and DEP was achieved in a single assay of *E. coli* detection performed on a single biochip. The significance of such an approach includes the following. First, EP is well suited for manipulating charged macromolecules whereas DEP is for manipulating large-sized bioparticles (micrometer or greater). The combined use exploits the advantages of both EP and DEP and provides an effective approach for detecting and assaying bioparticles. Second, EP and DEP can be performed with the same set of electrodes under different signal excitations. Such a method is particularly applicable to bioelectronic chips, where the individually addressable electrode array allows flexible and versatile application of EP and DEP in many different bioanalytical processes<sup>18-21,35</sup> including cell enrichment and separation, target concentration, and electric field-driven DNA hybridization and immunoassays. Finally, because different bioparticles (e.g., bacteria versus spores) can have different dielectric properties and as a consequence respond to an applied ac field differentially, direct incorporation of DEP for selectively manipulating target bioparticles in a bioassay provides additional specificity.

## CONCLUSIONS

We have demonstrated that electric field-based methods can be used to manipulate bioparticles on microelectronic chips for different applications, such as microscale separation, enrichment, and collection of micrometer-sized particle and macromolecules (e.g., antibodies) onto electrodes. By using dc and ac fields, both electrical charges and dielectric properties of particles are exploited for particle selective manipulation. In particular, a given

(35) Ewalt, K. L.; Haigis, R. W.; Rooney, R.; Ackley, D.; Krihak, M. *Anal. Biochem.* **2001**, *289*, 162-172.

(36) Ewalt, K. L.; Haigis, R. W., unpublished observations.



target bioparticle type can be specifically extracted and concentrated from a population of potentially interfering molecules or particles through the choice of particle suspension conductivity and applied field frequencies. Furthermore, we demonstrated an effective DEP enrichment of bioparticles from a diluted suspension. Finally, we provided novel electric field-driven immunoassays for detecting spores and bacteria by using dc and ac fields. For the first time, the combined use of EP and DEP was achieved in a single assay performed on a single chip, where EP was used for manipulating charged macromolecules (e.g., antibodies) and DEP for manipulating micrometer-sized bioparticles (e.g., bacteria). Besides the utilization of capture and detecting antibodies, such electric field-mediated assays have additional specificity, since different target bioparticles often respond to different ac frequencies. Consequently, we have developed a versatile technique for electric field-based separations and immunoassays on microelectrodes where ac, dc, or a combination of applied fields may be

incorporated with or without antibody-enhanced capture for different processes in micro analytical systems.

#### ACKNOWLEDGMENT

We thank Janice Bell, Paul Swanson, and Joon Mo Yang for valuable discussion. Special thanks to Dr. James Fan for the SDA experiment. We are grateful to Drs. Richard R. Anderson, Bruce Wallace, and Xiao Xu and for reading the manuscript and providing valuable comments. This work is supported by a research contract from the Microsystems Technology Office of the Defense Advanced Research Program Agency (DARPA/SPAWAR Contract N66001-98-C-8625).

Received for review September 15, 2000. Accepted January 18, 2001.

AC001109S